Eur. Phys. J. D **43**, 261–266 (2007)
DOI: 10.1140/epjd/e2007-00125-6

THE EUROPEAN PHYSICAL JOURNAL D

The effect of volumetric weighting in the interaction of intense laser fields with clusters

T. Döppner[a], J.P. Müller, A. Przystawik, J. Tiggesbäumker, and K.-H. Meiwes-Broer

Institute of Physics, University of Rostock, Universitätsplatz 3, 18051 Rostock, Germany

Received 10 December 2006 / Received in final form 28 December 2006
Published online 24 May 2007 –

Abstract. Silver clusters embedded in helium nanodroplets are exposed to intense femtosecond laser pulses (10^{13}–10^{16} W/cm^2). The signal of highly charged ($q \leq 11$) atomic fragments is maximized by delayed plasmon enhanced ionization using stretched laser pulses. Further details with respect to the dynamics of the charging process can be obtained, when the intensity distribution within the laser focus is taken into account. For the first time, the z-scan method is applied to clusters which offers a route to investigate the explicit dependence of the ion signals with respect to the laser intensity. By taking advantage of the volumetric weighting effect ionization thresholds are determined, yielding values well below 10^{14} W/cm^2 for Ag^{q+} ions with $q \leq 11$.

PACS. 36.40.Gk Plasma and collective effects in clusters – 52.50.Jm Plasma production and heating by laser beams (laser-foil, laser-cluster, etc.) – 36.40.Wa Charged clusters

1 Introduction

The interaction of nanosized objects with intense femtosecond laser pulses has developed to an area of active research, motivated both by fundamental questions and possible applications, e.g., as sources of EUV and X-ray radiation [1,2] or of highly charged atomic ions [3–6]. To date it is widely accepted that in the strong non-linear excitation regime the coupling of light into particles can be strongly enhanced by the excitation of the plasmon, which is the collective electron dipole resonance of a metallic system [4,7–11]. Due to the huge efficiency of the resonant charging ions with recoil energies up into the MeV regime can be produced [5,6]. Also there is evidence that the highest kinetic energies of the emitted electrons originate from ionization of the particles at resonance [12–14]. According to the well-known Mie-formula the plasmon energy depends on the ionic density as $\hbar\omega_{Mie} = \hbar\sqrt{e^2 n_i/3\epsilon_o m_e}$. Since in the clusters ground state n_i is usually too high for the laser frequency to match the eigenfrequency of the collective excitation, an expansion of the system is necessary. This can be triggered by a weak charging of the particle. When the density has reduced to a critical value, delayed plasmon enhanced ionization becomes possible. Typical time scales range from a few hundred femtoseconds up to several picoseconds, depending on the chosen cluster size and the applied laser intensity. In order to achieve delayed plasmon enhanced ionization several methods have been applied, i.e. the variation of the laser pulse width [2,4,15,16], dual pulse excitation [15,17], and a feedback algorithm [18].

With stretched laser pulses, even when the pulse energy is kept constant, an enhanced charging of the clusters can be obtained compared to an excitation with the shortest and thus most intense pulse. This was demonstrated by us in an earlier experiment on platinum clusters where atomic fragment charge states of up to $q = 20$ were produced [4]. However, only the dependence of the maximum charge on the pulse width was analyzed in detail. Recently, we have performed a charge selective study for ions resulting from silver clusters subject to dual pulse excitation [19]. One important result was, that the pulse separation to optimize the ion yield strongly depends on the charge state under consideration. It was proposed, that this is due to the interaction of the clusters with the light field in different regions of the laser focus, i.e. the charging dynamics is measured for different laser intensities simultaneously.

Up to now, only a few experiments have investigated the intensity dependence of the cluster charging process. In the majority of the studies usually only the peak intensity is given, and values in excess of 10^{15} W/cm^2 are reported. Only recently there is evidence that laser fields on the order of 10^{14} W/cm^2 are sufficient for giant charging of clusters [17,20]. In an experiment with rare gas clusters the group of Vernhet measured the emission of hard X-rays integrated over the whole laser focus [20]. The laser intensity was varied by changing the pulse energy, similar to the early experiments on the optical field ionization of single atoms, see e.g. [21]. Evidence was found that Ar^{q+}-ions

[a] e-mail: tilo.doeppner@uni-rostock.de

with up to $q = 16$ are generated with laser intensities as low as $3{\times}10^{14}\,\mathrm{W/cm^2}$. To explain the, compared to single atoms, hugely reduced ionization thresholds Deiss et al. have performed mean-field classical transport simulations and propose elastic large-angle backscattering of electrons at ionic cores in the presence of a laser field as an efficient heating mechanism [22]. Very recently the generation of multiply charged ions from Coulomb exploding $(CH_3I)_n$ clusters excited by nanosecond laser pulses having intensities as low as $10^9\,\mathrm{W/cm^2}$ was reported [23]. The authors rationalize their findings by the concept of energy pooling which becomes possible through the excitation of a long living state of the CH_3I molecule.

In this contribution we will use intensity selective scanning (ISS) [24] in order to determine threshold intensities in the interaction of silver clusters with intense light fields. What complicates the investigation of the intensity dependence is the problem of spatial averaging inherent in experiments with strong laser fields. In order to achieve high laser intensities, the light pulse has to be focused by a lens or a parabolic mirror, yielding a spatial intensity distribution

$$I(r,z) = \frac{I_o}{1+z'^2}\exp\left(-\frac{2r^2}{\omega_o^2(1+z'^2)}\right), \qquad (1)$$

with I_o the spatially and temporally overall peak intensity, $z' = \lambda z/\pi\omega_o^2$ and ω_o the beam waist radius. The resulting signal S at a particle or light detector in the experiment is thus always an average over a certain intensity range. Moreover, lower intensities occupy larger volumes compared to values close to the peak intensity. Due to this *volumetric weighting effect*, a signal which is generated with only a weak probability in the low intensity wings of the laser focus can become comparable or even dominating compared to that from the peak intensity region, possibly complicating the investigation of the explicit laser intensity dependence. For a gas of atoms it has been shown that it is possible to reduce the effect of volumetric weighting if one restricts the interaction region to only a slice of the laser focus oriented perpendicular to the light propagation axis. Several experimental approaches have been reported [24–26], e.g., a narrow slit is placed between the interaction region and the detector [24,25]. By varying the focus spot position with respect to the slit position over a sufficient z-range, it is possible to retrieve the laser intensity dependence of a certain process. Using this procedure it was possible to determine ionization rates for Xe^{q+} ions with up to $q = 4$ [24,27]. Recently, Benis et al. [26] have applied an imaging setup to measure the z-scan signal in a single-shot configuration. We wish to emphasize, that the z-scan method is not restricted to strong field phenomena. It can readily be adapted to related investigations like, e.g., ionization mass spectrometry with low fragmentation for structural analysis of biological systems, see e.g. [28].

Here we will demonstrate that the volumetric weighting effect is important for the interaction of clusters with intense femtosecond laser fields. In a charge selective study the strong field ionization of silver clusters embedded into helium nanodroplets is investigated. Excitation with stretched pulses is chosen as a complementary method to dual pulses used in reference [19] to corroborate the hypothesis found there. The z-scan method will be applied to determine intensity thresholds for high-q atomic ion fragments.

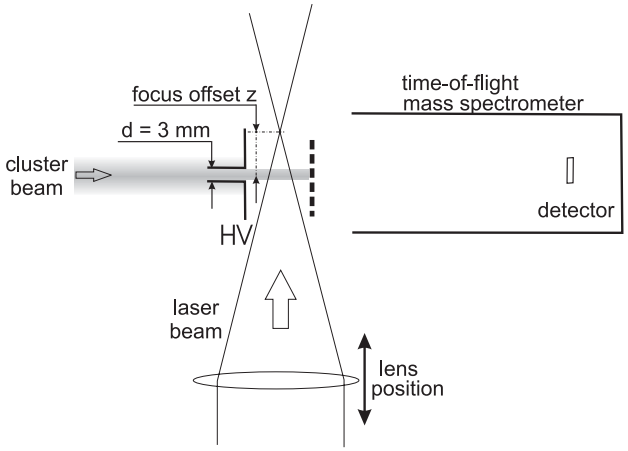

Fig. 1. Experimental geometry for the z-scan setup (dimensions are not to scale). The laser intensity in the interaction region is scanned by moving a $f = 40\,\mathrm{cm}$ focusing lens. By pulsing the repeller plate with high voltage (HV) the ions are accelerated towards the mass spectrometer. The width of the z-slice of the laser focus mapped towards the detector is determined by the diameter of the cluster beam ($d = 3\,\mathrm{mm}$). When the beam waist of the laser focus coincides with the molecular beam axis, i.e. the focus offset is $z = 0\,\mathrm{cm}$, the interaction volume reaches a minimum.

2 Experimental setup

For cluster generation the atom pick-up method is used to grow silver clusters inside helium nanodroplets. Details of the experimental apparatus are given in reference [29]. Briefly, the droplet beam is produced by means of a supersonic expansion of purified helium gas (He 6.0) at a stagnation pressure of 20 bar through a 5 μm nozzle which can be cooled down to 8.0 K. Under these source conditions the droplets consist of up to 10^7 helium atoms, and exhibit interesting properties like superfluidity, and an ultra-low temperature of 0.37 K, see e.g. [30]. In the pick-up chamber silver atoms are successively loaded into the droplets and form clusters with up to 150 atoms [31]. The clusters enter the interaction region through a 1 cm long tube which limits the diameter of the molecular beam to $d = 3\,\mathrm{mm}$, see Figure 1. This determines the slice of the laser focus which is mapped onto the detector. For excitation, a Ti:sapphire chirped pulse amplification system delivers 100 fs laser pulses with up to 25 mJ at 800 nm. The pulse width can easily be adjusted to more than 10 ps by detuning the compressor. The laser light perpendicularly propagating to the cluster beam is focused by a 40 cm lens ($f/33$), yielding a peak intensity of up to $5\times10^{16}\,\mathrm{W/cm^2}$, and a Rayleigh range of $z_R = 1.2\,\mathrm{mm}$. An adjustment of

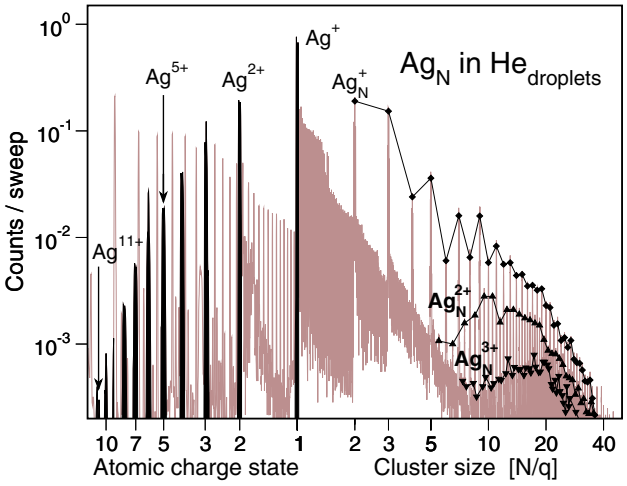

Fig. 2. Fragment spectrum of Ag_N ($\overline{N} = 40$) embedded in helium droplets exposed to 400 fs pulses, yielding an intensity of up to 3.9×10^{13} W/cm^2 at 800 nm. The signals from highly charged atomic fragment ions (Ag^{q+}) are highlighted and will be analyzed in detail. Clusters irradiated in the low intensity regions of the laser focus partly survive and give rise to signals of singly and multiply charged cluster ions (Ag_N^{q+}). Peaks corresponding to the same ionization state of a cluster are connected.

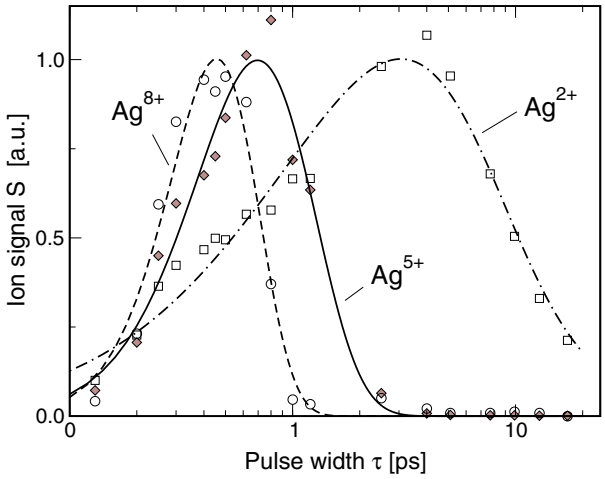

Fig. 3. Laser pulse width dependence of the ion yield for selected Ag^{q+} fragments, when irradiating silver clusters with 15 mJ pulses at 800 nm, integrated over 6000 laser shots. For the shortest pulse of 130 fs the peak intensity is $I_o = 1.2 \times 10^{14}$ W/cm^2. Note, that towards larger pulse widths the maximum laser intensity during the pulse decreases. The data are normalized for better comparison, and the fit curves serve as a guide to the eye.

the laser intensity is accomplished by shifting the position of the laser focus with respect to the cluster beam axis. The resulting products of the interaction process are analyzed by a time-of-flight mass spectrometer having a resolution of $m/\Delta m = 2000$.

3 Results and discussion

Upon excitation the silver clusters disintegrate, leading to a richly structured fragment distribution. A typical mass spectrum is shown in Figure 2. For this measurement the lens position was chosen such that the center of the laser focus is well separated from the molecular beam axis, yielding a peak intensity of only 3.9×10^{13} W/cm^2 in the interaction region. Even though this value is well below the overall peak intensity in the laser focus, atomic ions with up to $q = 11$ from Coulomb exploding clusters are detected. Higher charged ions might be generated but can not be measured due to a strong signal of He_2^+. At longer flight times, corresponding to higher N/q ratios, in the mass spectrum appear singly and multiply charged cluster ions. A series of Ag_N^{2+} and Ag_N^{3+} can unambiguously be identified. In addition to the signals from Ag_N^{q+}, abundance distributions of ion-snowball complexes $Ag^{q+}He_N$ ($q = 1, 2$, $N = 1 \ldots 150$) are detected [32]. Since clusters can only survive the interaction process when exposed to the laser field in the low intensity region of the focus, the appearance of larger fragments gives a first hint that a wide laser intensity range is mapped to the detector. For the rest of this contribution we will concentrate on the highly charged atomic ions.

3.1 Pulse width dependence

Mass spectra as shown in Figure 2 are measured with respect to the pulse width τ, keeping the pulse energy constant. Those channels of the spectrum which can be assigned to a certain charge state q are integrated and plotted with respect to τ. Figure 3 presents an example of such an analysis for selected q. A signal from multiply-charged atomic ions is obtained for pulses having a width of up to 20 ps. All Ag^{q+} show a strong dependence on τ with a distinct abundance maximum for a certain pulse width. The general phenomenon of an optimum pulse width is well-known and reflects the effect of delayed plasmon enhanced ionization [4]. However, up to now only minor attention has been paid to the fact that the optimum pulse width τ_{max} strongly depends on the considered ionization state. In this investigation we found values ranging from 450 fs (Ag^{11+}) to 6.5 ps (Ag^+), see Figure 4. The lowest value of τ_{max} is found for the highest q. To understand this behavior it is helpful to analyze the signals $S_{max}(q)$ associated with $\tau_{max}(q)$. The result is shown in the inset of Figure 4. With the exception of the singly charged ion a clear exponential decrease is found as a function of q, visualized by the straight line. The enhanced abundance of Ag^+ might be due to ionization of bare silver atoms which are emitted from the oven in the pick-up cell and drift into the interaction region. The distinct drop of S_{max} towards higher charge states implies that the detected atomic ions originate from different intensity regions of the laser focus slice defined by the cluster beam. Note that due to the volumetric weighting effect the volume occupied by a certain laser intensity interval is inversely proportional to the intensity (cf. Eq. (1)). Under the reasonable assumption that higher atomic charge states are generated in regions

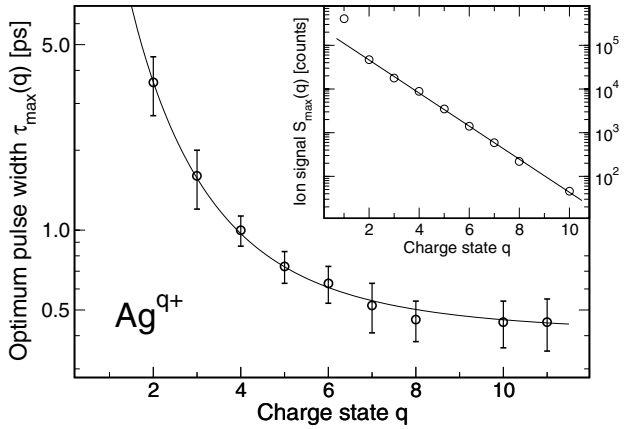

Fig. 4. Laser pulse widths τ_{max} which maximize the Ag^{q+}-signals, extracted from the measurement shown in Figure 3. The data points are fitted to a $1/z^{2.5}$ function which serves as a guide to the eye only. Inset: absolute ion yields $S_{max}(q)$ obtained with the corresponding optimum pulse width $\tau_{max}(q)$. $S_{max}(q)$ decreases exponentially as a function of q indicating that each q is preferentially generated in a different region of the laser focus.

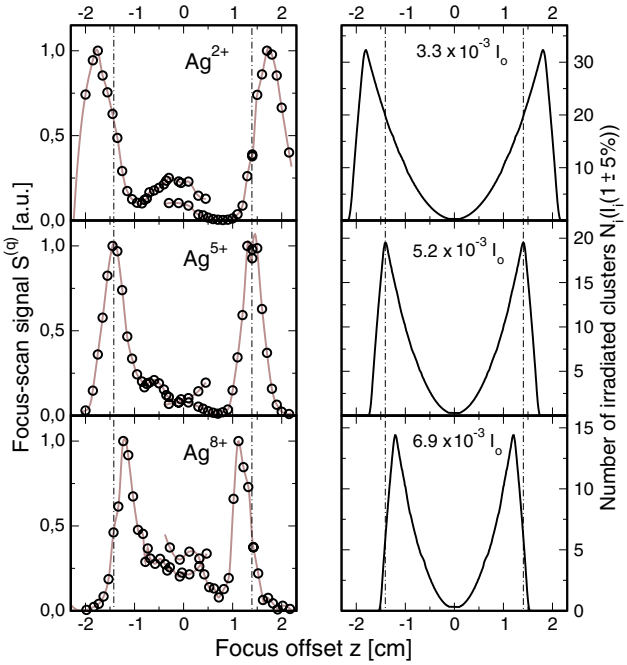

Fig. 5. Left: focus scan signal of selected Ag^{q+} fragments when irradiating Ag_N embedded in helium droplets with 13 mJ pulses of $\tau = 300$ fs at 800 nm, yielding a peak intensity of $I_o = 9.0 \times 10^{15}$ W/cm^2. The solid curves serve as a guide to the eye. The vertical lines mark the position of the maxima obtained for Ag^{5+}. Right: calculated number of clusters per laser shot exposed to selected laser peak intensities $I_i \pm 5\%$. A double-peak profile is obtained in the experiment as well as in the calculation indicating that the degree of ionization of the atomic fragment ions depends on the position of the cluster in the laser focus. For further details, see text.

of stronger laser fields the q-dependence of τ_{max} can be explained. Lower intensities in the outer wings of the focus result in a lower initial ionization of the cluster compared to particles closer to the center of the focus. This leads to a slower cluster expansion, thus the whole process decelerates and τ_{max} shifts to a larger value. In addition, the peak intensity at resonance is lowered due to the temporally stretched pulse, reducing the final charging. A similar behavior has been found for the optimum *delay* in an experiment with dual pulse excitation [19]. In order to verify the argumentation above we now apply the z-scan method to obtain a relationship between the atomic charge state and the laser intensity necessary to generate the considered charge state.

3.2 Focus scan measurement

To perform the z-scan, the focus offset as defined in Figure 1 is systematically varied. For excitation a pulse width of 300 fs was used, ensuring both an intense laser field of up to 9.0×10^{15} W/cm^2 and the efficient generation of the highest charged ions, cf. Figure 3. Spectra as shown in Figure 2 were recorded at a number of z-positions. Due to the limited range of the translation stage two overlapping z-scans were performed and the maxima of both curves were separately normalized. Using the signals of all multiply-charged ions, the position of $z = 0$ cm was deduced, i.e. the lens position at which the center of the laser focus coincides with the molecular beam axis. The extracted signals of selected ionic charge states are plotted in Figure 5 (left). Interestingly, at $z = 0$ cm only a low yield of Ag^{q+} is obtained for all charge states $q > 1$. When increasing the focus offset the multiply-charged ion signal strongly rises and distinct maxima are found symmetrically on both sides of $z = 0$ cm, e.g., at $z_{max} = \pm 1.41$ cm for Ag^{5+}. No ions are detected beyond a focus offset of 2.5 cm for $q \geq 3$. In addition, the measured signals reveal a trend with respect to q. The optimum focus offset z_{max} shifts towards smaller z with increasing charge state. This implies a distinct relationship between the probability to generate a certain charge state and the laser intensity, and clearly reflects the effect of the volumetric weighting.

In the following we will describe a simple procedure to obtain q-specific threshold intensities I_{th} from the z-scan signals shown in Figure 5. The Ag^{q+} ion signal S depends on the (volume independent) count rate $\gamma^{(q)}(I)$ of the charge state q, the number of irradiated clusters $N(I, z)$ at a given intensity I and a focal offset z, as well as the focal intensity distribution:

$$S^{(q)}(z) \propto \int_0^{I_o} \gamma^{(q)}(I)\, N(I, z)\, dI. \qquad (2)$$

It can be expected that $\gamma^{(q)}(I)$ will rise sharply at a threshold intensity $I_{th}^{(q)}$, for which the system can absorb enough energy to produce the charge state q. In order to perform a quantitative analysis of the experimental results we make the simplified assumption that $\gamma^{(q)}(I)$ only has

significant contributions in the threshold region, i.e.

$$\gamma^{(q)}(I) = \begin{cases} const. & I \in [I_{th}^{(q)} \pm \Delta I] \\ 0 & I \notin [I_{th}^{(q)} \pm \Delta I] \end{cases} . \quad (3)$$

The width of the intensity interval was chosen such that $\Delta I / I_{th} = 0.05$. Under these assumptions equation (2) reduces to

$$S^{(q)}(z) \propto N\left(I_{th}^{(q)}(1 \pm 5\%), z\right). \quad (4)$$

In order to make quantitative assignments to the measured focus scan signals the number of clusters which are irradiated with different laser intensities $N_i(I_i(1\pm5\%), z)$ is estimated with respect to the focus offset z. A Gaussian laser focus (Eq. (1)) is assumed as well as a homogeneous target density. Results with the best matching to the corresponding experimental signal $S^{(q)}$ are plotted in the right column of Figure 5. As in the experiment, the distinct double peak structure symmetric with respect to $z = 0\,\mathrm{cm}$ very distinctly shows the effect of volumetric weighting. The good accordance of this simplified approximation with the experimental data gives a strong hint that clusters irradiated at low intensities around $I_{th}^{(q)}$ yield the main fraction of the ion signal $S^{(q)}$ at the detector. Moreover, the pronounced structure with two narrow peaks, especially of the Ag^{5+} and Ag^{8+} signals, suggests that the majority of differently charged ions originates from spatially separated regions of the laser focus.

Up to now a very simple form of $\gamma^{(q)}(I)$ was assumed, cf. equation (3). If there were additional non zero contributions to $\gamma^{(q)}(I)$ for $I < I_{th}^{(q)}$ than the calculated signals would be significantly broadened to larger focus offsets. Due to the volumetric weighting effect the number of irradiated clusters increases to lower laser intensities, e.g., by a factor of two when considering $N(I = 3.3 \times 10^{-3} I_o$, $z = 1.76\,\mathrm{cm})$ compared to $N(I = 6.9 \times 10^{-3} I_o$, $z = 1.18\,\mathrm{cm})$, cf. Figure 5. Thus, assuming the volume independent count rate $\gamma^{(q)}(I)$ would be the same in two different laser intensity intervals, clusters in the lower intensity interval would generate a larger fraction of the signal at the detector. Therefore, the assignments made in Figure 5 can indeed be interpreted as intensity thresholds $I_{th}^{(q)}$ to create Ag^{q+}, i.e. $\gamma^{(q)}(I)$ increases sharply at the intensities extracted from Figure 5 and summarized in Table 1.

The interpretation of the experimental data at small focus offsets, i.e. at higher laser intensities, is more complicated. Assuming $\gamma^{(q)}(I) \approx \gamma^{(q)}(I_{th})$ for $I > I_{th}$ would just lead to a broadening of the two peaks towards lower z. Our simulations indicate that additional structure as observed for Ag^{2+} around $z = 0\,\mathrm{cm}$ appears if γ increases with laser intensity or additional processes like the ionization of bare atoms take place. Even though it is a challenging task, the complete deconvolution of $\gamma^{(q)}(I)$ from the experimental data $S^{(q)}(z)$ is possible, as was shown in references [27,33,34] for optical field ionization of atoms. In clusters the situation might be even more complex since additionally fragmentation of the multiply charged clusters, electron-ion recombination and charge transfer within the dense target certainly play a role. Therefore, here we will restrict the discussion to the threshold intensity necessary to bring atoms of a cluster into a certain charge state.

The most astonishing result of the current investigation is that the generation of Ag^{q+} ions up to $q = 11$ starts already for laser intensities well below $10^{14}\,\mathrm{W/cm^2}$. This is more than two orders of magnitude below the overall peak intensity used in this experiment. For comparison, to ionize a bare silver atom to $q = 11$ by optical field ionization, an intensity of $4.3 \times 10^{16}\,\mathrm{W/cm^2}$ is necessary [21]. We note, that our experiments were performed with silver clusters embedded in helium droplets. Even though helium is transparent for 800 nm radiation, it might act as a reservoir for additional electrons and thus enhancing the heating by inverse bremsstrahlung. The influence of the helium surrounding on the charging dynamics has not been completely clarified yet, and is a topic of current research. Due to the process of delayed plasmon enhanced ionization, in the case of clusters not only the pulse intensity but also the temporal profile of the laser field is important. For instance, in the present z-scan study the pulse width of 300 fs was not optimized for the generation of weakly charged ions like Ag^{2+}, see Figure 3. Thus, by applying the appropriate pulse widths, even lower thresholds for these charge states might be conceivable, not disrupting, however, the observed qualitative behavior. For a detailed analysis of how the effect of plasmon enhanced ionization influences the ionization thresholds, both methods presented in this contribution, i.e. excitation with stretched laser pulses and the z-scan method, have to be combined more systematically.

Table 1. Intensity thresholds to generate selected Ag^{q+} ions when irradiating silver clusters with 300 fs laser pulses, extracted from the z-scan measurement shown in Figure 5.

charge state q	optimum focus offset $z_{max}(q)$ [cm]	threshold intensity $I_{th}^{(q)}$ [W/cm^2]
2	1.76 ± 0.02	3.0×10^{13}
5	1.41 ± 0.02	4.7×10^{13}
8	1.18 ± 0.02	6.2×10^{13}

4 Conclusion

The effect of delayed plasmon enhanced ionization in the charging of silver metal clusters embedded in helium nanodroplets and exposed to intense laser fields was demonstrated. To optimize the yield of a certain fragment ion charge state at a given pulse energy, the pulse width had to be adjusted and values between 460 fs and 3.6 ps were obtained for Ag^{8+} and Ag^{2+}, respectively. Evidence was found that a wide range of laser intensities is simultaneously probed and mapped onto the ion detector. The z-scan method was applied to charging of clusters in strong laser fields. Due to the effect of volumetric weighting this method is well suited to determine charge specific intensity thresholds. The extremely low values below

$10^{14}\,\mathrm{W/cm^2}$ clearly show the outstanding position of small particles in the ionization of matter in intense laser fields.

We are obliged to J.P. Toennies and his group from the Max Planck Institut in Göttingen who constructed and built the helium droplet machine. Financial aid by the Deutsche Forschungsgemeinschaft through the Sonderforschungsbereich 652 is gratefully acknowledged.

References

1. A. McPherson, B.D. Thompson, A.B. Borisov, K. Boyer, C.K. Rhodes, Nature **370**, 631 (1994)
2. E. Parra, I. Alexeev, J. Fan, K.Y. Kim, S.J. McNaught, H.M. Milchberg, Phys. Rev. E **62**, R7603 (2000)
3. E.M. Snyder, S.A. Buzza, A.W. Castleman Jr, Phys. Rev. Lett. **77**, 3347 (1996)
4. L. Köller, M. Schumacher, J. Köhn, S. Teuber, J. Tiggesbäumker, and K.-H. Meiwes-Broer, Phys. Rev. Lett. **82**, 3783 (1999)
5. T. Ditmire, J.W.G. Tisch, E. Springate, M.B. Mason, N. Hay, R.A. Smith, I. Marangos, M.M.R. Hutchinson, Nature **386**, 54 (1997)
6. M. Lezius, S. Dobosz, D. Normand, M. Schmidt, Phys. Rev. Lett. **80**, 261 (1998)
7. E. Suraud, P.G. Reinhard, Phys. Rev. Lett. **85**, 2296 (2000)
8. J. Daligault, C. Guet, Phys. Rev. A **64**, 043203 (2001)
9. U. Saalmann, J.-M. Rost, Phys. Rev. Lett. **91**, 223401 (2003)
10. Th. Fennel, K.-H. Meiwes-Broer, G.F. Bertsch, Eur. Phys. J. D **29**, 367 (2004)
11. U. Saalmann, C. Siedschlag, J.-M. Rost, J. Phys. B **39**, R39 (2006)
12. E. Springate, S.A. Aseyev, S. Zamith, M.J.J. Vrakking, Phys. Rev. A **68**, 053201 (2003)
13. V. Kumarappan, M. Krishnamurthy, D. Mathur, Phys. Rev. A **67**, 043204 (2003)
14. T. Döppner, Th. Fennel, P. Radcliffe, J. Tiggesbäumker, K.-H. Meiwes-Broer, Phys. Rev. A **73**, 031202(R) (2006)
15. J. Zweiback, T. Ditmire, M.D. Perry, Phys. Rev. A **59**, R3166 (1999)
16. K.J. Mendham, J.W.G. Tisch, M.B. Mason, N. Hay, J.P. Marangos, Opt. Expr. **11**, 1357 (2003)
17. T. Döppner, Th. Fennel, Th. Diederich, J. Tiggesbäumker, K.-H. Meiwes-Broer, Phys. Rev. Lett. **94**, 013401 (2005)
18. S. Zamith, T. Martchenko, S.A. Aseyev, H.G. Muller, M.J.J. Vracking, Phys. Rev. A **70**, 011201 (2004)
19. T. Döppner, Th. Fennel, P. Radcliffe, J. Tiggesbäumker, K.-H. Meiwes-Broer, Eur. Phys. J. D **36**, 165 (2005)
20. E. Lamour, C. Prigent, J.P. Rozet, D. Vernhet, Nucl. Instrum. Meth. Phys. Res. B **235**, 408 (2005)
21. S. Augst, D. Strickland, D.D. Meyerhofer, S.L. Chin, J.H. Eberly, Phys. Rev. Lett. **63**, 2212 (1989)
22. C. Deiss, N. Rohringer, J. Burgdörfer, E. Lamour, C. Prigent, J.-P. Rozet, D. Vernhet, Phys. Rev. Lett. **96**, 013203 (2006)
23. P. Sharma, R.K. Vatsa, S.K. Kulshreshtha, J. Jha, D. Mathur, M. Krishnamurthy, J. Chem. Phys. **125**, 034304 (2006)
24. P. Hansch, M.A. Walker, L.D. Van Woerkom, Phys. Rev. A **54**, R2559 (1996)
25. W.A. Bryan, S.L. Stebbings, J. McKenna, E.M.L. English, M. Suresh, J. Wood, B. Srigengan, I.C.E. Turcu, J.M. Smith, E.J. Divall, C.J. Hooker, A.J. Langley, J.L. Collier, I.D. Williams, W.R. Newell, Nature Phys. **2**, 379 (2006)
26. E.P. Benis, J.F. Xia, X.M. Tong, M. Faheem, M. Zamkov, B. Shan, P. Richard, Z. Chang, Phys. Rev. A **70**, 025401 (2004)
27. T.R.J. Goodworth, W.A. Bryan, I.D. Williams, W.R. Newell, J. Phys. B **38**, 3083 (2005)
28. S.M. Hankin, D.M. Villeneuve, P.B. Corkum, D.M. Rayner, Phys. Rev. Lett. **84**, 5082 (2000)
29. A. Bartelt, J.D. Close, F. Federmann, N. Quaas, J.P. Toennies, Phys. Rev. Lett. **77**, 3525 (1996)
30. Special issue on helium droplets, J. Chem. Phys. **115**, 10065-10281 (2001)
31. P. Radcliffe, A. Przystawik, Th. Diederich, T. Döppner, J. Tiggesbäumker, K.-H. Meiwes-Broer, Phys. Rev. Lett. **92**, 173403 (2004)
32. T. Döppner, Th. Diederich, S. Göde, A. Przystawik, J. Tiggesbäumker, K.-H. Meiwes-Broer, J. Chem. Phys. (submitted)
33. M.A. Walker, P. Hansch, L.D. Van Woerkom, Phys. Rev. A **57**, R701 (1998)
34. W.A. Bryan, S.L. Stebbings, E.M.L. English, T.R.J. Goodworth, W.R. Newell, J. McKenna, M. Suresh, B. Srigengan, I.D. Williams, I.C.E. Turcu, J.M. Smith, E.J. Divall, C.J. Hooker, A.J. Langley, Phys. Rev. A **73**, 013407 (2006)